A realistic and easy-to-implement weighting model for GPS phase observations

X. Luo[a,*], M. Mayer[a], B. Heck[a], J. L. Awange[a,b]

[a] *Geodetic Institute, Karlsruhe Institute of Technology (KIT), Englerstraße 7, 76131 Karlsruhe, Germany*

[b] *Western Australian Centre for Geodesy and Institute for Geoscience Research, Curtin University, GPO Box U1987, WA 6845 Perth, Australia*

Abstract

Observation weighting is an essential component of the GPS stochastic model and plays a key role in reliable outlier detection and parameter estimation. Nowadays, satellite elevation angle and signal-to-noise ratio (SNR) are used as quality indicators for GPS phase measurements in high-accuracy geodetic applications. In comparison to elevation-dependent models, SNR-based weighting schemes represent the reality better, but usually require greater implementation efforts. Relying upon a representative analysis of empirical SNR-based weights, this paper proposes an elevation-dependent exponential weight function EXPZ, which benefits from realistic SNR-based weights and enables easy software implementation. To process GPS data from a regional network, this advanced weighting scheme is implemented in the Bernese GPS Software 5.0 and compared with the conventional elevation-dependent COSZ model in terms of phase ambiguity resolution, troposphere parameter esti-

*Corresponding author

Email addresses: xiaoguang.luo@kit.edu (X. Luo), michael.mayer@kit.edu (M. Mayer), bernhard.heck@kit.edu (B. Heck), J.Awange@curtin.edu.au (J. L. Awange)

mation, and site coordinate determination. The results show that the proposed EXPZ model significantly attenuates the downweighting effects on low-elevation observations and improves the success rates of ambiguity resolution by about 10%, the standard deviations of site-specific troposphere parameters by about 40%, and the repeatabilities of daily coordinate estimates by up to 2.3 mm (50%).

Keywords: GPS; Stochastic model; Observation weighting; Satellite elevation angle; Signal-to-noise ratio (SNR)

---

1. Introduction

Weighting GPS measurements, which allows the user to specify observational contributions to an overall solution, is necessary for reliable GPS data analysis. This simply arises from the fact that GPS observations from different satellites at different epochs have different degrees of precision, e.g., due to different atmospheric effects. Accordingly, a precise measurement should contribute more to parameter estimation and have a larger weight than an imprecise one.

The importance of appropriate weighting methods has been realised long ago, e.g., by Teunissen et al. (1998). They stated that the least-squares method, which is widely applied in GPS data processing, will lose its property of minimum variance if a misspecified weighting scheme is used. Furthermore, the power of the statistical tests employed for model validation and quality control (e.g., outlier and cycle slip detection) is significantly reduced if the noise characteristics are not properly considered (Kim and Langley, 2001; Wieser and Brunner, 2002). In addition, any misspecification in ob-

servation weighting will inevitably produce biased parameter estimates and overly optimistic accuracy measures (Howind, 2005, Sect. 5.3.3; Schön and Brunner, 2008). For example, applying an identical weight of $w = 1$ to all observations is inadequate for high-precision GPS applications, particularly when including low-elevation data (Bischoff et al., 2005; Luo et al., 2007; Satirapod and Luansang, 2008; Amiri-Simkooei et al., 2009). In spite of its importance, a realistic observation weighting model, which sufficiently copes with receiver and antenna characteristics, signal strength, multipath and atmospheric effects, etc., still remains a difficult task (Wieser, 2007).

Instead of an equal weight, the satellite elevation angle is often used as a quality indicator for GPS observations. The basic idea is that measurements at lower elevation angles suffer more strongly from atmospheric and multipath effects, hence are noisier. Also, receiver antenna gain is typically less at lower elevation angles, leading to lower signal quality. Under weak multipath and calm atmospheric conditions, the relationship between observation precision and elevation angle can be adequately described by cosecant (King and Bock, 2002, Chap. 5, pp. 9, 12; Dach et al., 2007, p. 144) or exponential (Euler and Goad, 1991; Han, 1997) functions. The main advantage of elevation-dependent weighting schemes is easy implementation. Therefore, they are widely used in GPS data processing software. However, for observations that are strongly affected by multipath effects, signal diffraction, and receiver characteristics, the elevation-dependent weighting concept becomes inappropriate. Moreover, it ignores the frequency-related differences in observation quality and downweights low-elevation data so that their contributions to parameter estimation are extremely limited (Wieser, 2007).

In addition to the satellite elevation angle, signal-to-noise ratio (SNR) was introduced as a more realistic quality indicator for GPS observations. Langley (1997) published a relationship between phase variances and SNR measurements, which was used to develop the SIGMA-ϵ and SIGMA-Δ models, coping with low-elevation data, signal diffraction, and multipath effects (Hartinger and Brunner, 1999; Brunner et al., 1999; Wieser and Brunner, 2000). However, the formula provided by Langley (1997) ignores any contribution to the noise characteristics from local oscillators and is only valid for relatively strong signals (Collins and Langley, 1999, p. 4). To overcome these deficiencies, Mayer (2006, p. 62) and Luo et al. (2008a,c) proposed empirical site-specific SNR-based weighting models, which properly deal with low-quality measurements of weak signals and sufficiently reflect variations in observation quality due to receiver properties, multipath effects, and atmospheric conditions. Being superior to the elevation-dependent weighting schemes, the SNR-based models realistically consider site-specific influences, appropriately handle low-elevation data, and directly produce frequency-related weights. Nevertheless, they suffer from the non-standardisation of SNR and the generally more complex software implementation (Collins and Langley, 1999, p. 4; Mayer, 2006, p. 59; Luo et al., 2008c; Joseph, 2010).

To combine the advantages of the elevation-dependent and SNR-based weighting concepts, this paper proposes a realistic and easy-to-implement weighting model for GPS phase observations. It makes use of the exponential function suggested by Euler and Goad (1991) and is denoted as EXPZ. The proposed approach is realistic, since it relies upon a representative analysis of empirical SNR-based weights and appropriately attenuates the downweight-

ing effects on low-elevation measurements. The EXPZ model can be easily implemented, as it depends only on the satellite elevation angle, which is used as an indicator for observation quality in many GPS software products.

The rest of this paper is organised as follows. In Sect. 2, the proposed EXPZ model is presented, along with a brief introduction of the underlying empirical SNR-based weighting scheme. Sect. 3 describes the case study and the GPS data analysis. In Sect. 4, the results of the case study are discussed with respect to (i) phase ambiguity resolution, (ii) troposphere parameter estimation, and (iii) site coordinate determination. Finally, Sect. 5 provides concluding remarks and an outlook on future research work.

2. Methodology

2.1. Empirical SNR-based weighting model (ESNR)

The underlying weighting model ESNR is completely independent from the variance function provided by Langley (1997) and is realised as follows. First, environment-specific signal quality measurements are extracted from RINEX observation files and, if necessary, converted into signal-to-noise power density ratio ($SNR0$ in dBHz) by means of model- and manufacturer-specific formulas (Collins and Stewart, 1999). The post-correlation quantity $SNR0$ refers to the ratio of the signal power and the noise power per unit bandwidth (Butsch, 2002), and can be considered as a synonym for carrier-to-noise density C/N_0 (Butsch and Kipka, 2004). Then, for each antenna-receiver combination (ARC) within the network, the minimum and maximum $SNR0$, denoted as $SNR0^{\min}_{ARC,i}$ and $SNR0^{\max}_{ARC,i}$ respectively, are searched over the entire period of investigation, where the subscript i denotes the carrier

frequency. Finally, the SNR-based weights are obtained using the minimum-related ratio between the actual $SNR0$ and the corresponding maximum. For the phase observation $\Phi^s_{R,i}(t)$ related to receiver R, satellite s, frequency i, and epoch t, the empirical SNR-based weight $w\left[\Phi^s_{R,i}(t)\right]$ is computed as

$$w\left[\Phi^s_{R,i}(t)\right] = \left[a + (1-a)\cdot\left(\frac{SNR0^s_{R,i}(t) - SNR0^{\min}_{ARC,i}}{SNR0^{\max}_{ARC,i} - SNR0^{\min}_{ARC,i}}\right)\right]^2. \qquad (1)$$

The parameter $a = 0.1$ prevents the singularity of the cofactor $q = w^{-1}$ if $SNR0^s_{R,i}(t) = SNR0^{\min}_{ARC,i}$, and is empirically determined as described in Luo (2013, Sect. 5.3.1). For representative antenna-receiver combinations, Fig. 1 compares the ESNR weighting scheme with the elevation-dependent COSZ model implemented in the Bernese GPS Software 5.0 (Dach et al., 2007, p. 144), i.e.,

$$w = \cos^2 z = \sin^2 e, \qquad (2)$$

where z and e denote the zenith distance and the satellite elevation angle, respectively. As Fig. 1a, c, and d show, in comparison to COSZ, the ESNR model reflects the differences in antenna-receiver combination and produces considerably larger weights for low- and medium-elevation measurements. Moreover, comparing Fig. 1a and b with each other, the frequency-related differences in observation quality can be taken into account when using ESNR, whereas they are completely ignored if COSZ is applied. For a more detailed discussion of ESNR, the reader is referred to Luo et al. (2008a,c) and Luo (2013, Chaps. 5 and 6).

FIGURE 1

141 *2.2. Exponential elevation-dependent weighting model (EXPZ)*

142 The proposed weighting model EXPZ relies upon the empirical SNR-
143 based weights calculated by Eq. (1) and makes use of the exponential function

$$\sigma^2 = \left[b_0 + b_1 \cdot \exp\left(\frac{-e}{e_0} \right) \right]^2, \tag{3}$$

145 where σ^2 denotes the variance of the phase measurement at elevation angle
146 e (Euler and Goad, 1991). Depending on the receiver type, the unknown
147 parameters b_0, b_1, and e_0 can be determined by applying the least-squares
148 method to elevation-dependent observation uncertainties (Euler and Goad,
149 1991; Han, 1997). Considering the variance in the zenithal direction as a
150 reference, i.e., $\sigma_0^2 = \sigma^2(e = 90^\circ)$, the weight for an individual phase measure-
151 ment is derived using

$$w = \frac{\sigma_0^2}{\sigma^2}. \tag{4}$$

153 In this paper, the model parameters of EXPZ are determined in an ad-hoc
154 manner by approximating the mean behaviour of the empirical SNR-based
155 weights (see Eq. (1)) from different case studies. Thereby, various aspects
156 were taken into account, such as antenna-receiver combination, observation
157 period, atmospheric conditions, and site-specific multipath effects (Luo et al.,
158 2008a,c; Luo, 2013, Chaps. 5 and 6). The parameter values for one-way
159 carrier-phase are $b_0 = 1.7$ mm, $b_1 = 3.3$ mm, and $e_0 = 40^\circ$ (see Eq. (3)). In
160 Fig. 2, the standard deviations (σ) and observation weights (w) produced by
161 the COSZ and EXPZ models are compared.

162 FIGURE 2

In terms of the σ values (see Fig. 2a), the proposed EXPZ model decreases much more slowly than COSZ for $e < 15°$, which attenuates the differences in observation quality at low elevation angles. As e increases from 5° to 80°, the EXPZ-related σ decreases from about 5 to 2 mm, coinciding with the phase accuracy estimates presented by Li et al. (2008) for different types of receivers. Regarding the observation weights shown in Fig. 2b, one can clearly discern that, in comparison to COSZ, the EXPZ curve exhibits significantly larger weights for low- and medium-elevation measurements, and lies below COSZ at high elevation angles. This sufficiently reflects the main elevation-dependent characteristics of the empirical SNR-based weights depicted in Fig. 1. Within the framework of this study, the EXPZ model is implemented in the Bernese GPS Software 5.0 (subroutine `WGTELV.f`; Dach et al., 2007, p. 144), and its effects on static relative positioning are examined using GPS data from a regional network.

3. Study area and GPS data analysis

The case study was carried out using 7 days of 30 s GPS data from a regional network that comprises three stations of the International GNSS Service (IGS) and one station of the Integrated German Geodetic Reference Network (GREF) (see Fig. 3). The IGS sites include Zimmerwald (ZIMM), Wettzell (WTZR), and Hügelheim (HUEG), while the GREF site BFO1 is located at the Black Forest Observatory (BFO) in southwest Germany (Luo and Mayer, 2008). The period of investigation is DOY2010:301–307, where DOY2010 denotes day of year 2010. The shortest and longest baselines shown in Fig. 3 are HUBF (HUEG → BFO1) and ZIWT (ZIMM → WTZR),

reaching about 77 and 476 km, respectively (see Table 1). The absolute difference in ellipsoidal height between two endpoints of a baseline, denoted as $|\Delta h|$ in Table 1, varies from 24.30 m (WTBF) to 678.03 m (ZIHU).

FIGURE 3

Table 1: Characteristics of the formed baselines (see Fig. 3).

Baseline	**From**[1]	**To**	**Length [km]**	$\lvert\Delta h\rvert$ **[m]**
HUBF	HUEG	BFO1	**77.4**	412.01
ZIHU	ZIMM	HUEG	106.9	**678.03**
ZIBF	ZIMM	BFO1	174.1	266.03
WTBF	WTZR	BFO1	346.9	**24.30**
WTHU	WTZR	HUEG	416.6	387.71
ZIWT	ZIMM	WTZR	**475.9**	290.32

[1] Reference site for baseline solution

Using the Bernese GPS Software 5.0, static relative positioning was performed by applying the observation weighting schemes COSZ and EXPZ. According to the previous finding that higher performance of the ESNR model can be reached by decreasing the elevation cut-off angle, e.g., from 10° to 3° (Luo et al., 2008a,c), a minimum elevation angle of 3° was chosen. Despite potentially stronger multipath effects, the use of low-elevation observations improves satellite geometry (Hartinger and Brunner, 1999) and decorrelates station height and troposphere parameter estimates (Dach et al., 2007, p. 247). In terms of external data and correction models, precise and up-to-date products were incorporated (see Table 2). The final daily and weekly solutions were obtained from stacking the normal equations in order to achieve a more sophisticated definition of the geodetic datum (e.g., minimum constraint solution; Dach et al., 2007, p. 216). In Table 2, important specifications of the GPS data analysis are listed.

206 Table 2: Important specifications of the GPS data analysis using the Bernese Software.

Geodetic datum	IGS05, epoch 2000.0
GPS observations	30 s phase double differences
Processing time interval	DOY2010:301–307 (daily/weekly solutions)
Observation weighting model	COSZ (see Eq. (2); Dach et al., 2007, p. 144) EXPZ (see Eqs. (3)–(4))
Elevation cut-off angle	3°
Satellite orbits/EOP[1]	Final IGS products (15 min/24 h)
Ionosphere model	Final CODE[2] products
Troposphere a priori model	Saastamoinen model (Saastamoinen, 1973)
Tropospheric mapping function	Niell mapping functions (Niell, 1996)
Time span of troposphere parameter	1 h
Time span of tropospheric gradient	24 h (Dach et al., 2007, p. 249)
Phase ambiguity resolution	SIGMA-dependent strategy (L5, L3)
Antenna correction model	IGS05 absolute model (Schmid et al., 2007)

[1] Earth orientation parameters
[2] Center for Orbit Determination in Europe

207 ## 4. Results and discussion

208 In comparison to the conventional COSZ weighting scheme, the effects of
209 the proposed EXPZ model on GPS parameter estimation were studied with
210 regard to phase ambiguity resolution, troposphere parameter estimation, and
211 site coordinate determination. While ambiguities are resolved in baseline
212 solutions, site-specific troposphere parameters and coordinates are obtained
213 from network solutions.

214 ### *4.1. Effects on phase ambiguity resolution*

215 Using the SIGMA-dependent algorithm provided by the Bernese GPS
216 Software 5.0 (Dach et al., 2007, Sect. 8.3.3), a two-step ambiguity (AMB)
217 resolution strategy is employed in this study (Dach et al., 2007, p. 182).
218 For each baseline presented in Table 1, the wide-lane (WL/L5) ambiguities
219 are first resolved by fixing all site coordinates, where the ionosphere model

from CODE is considered. Next, the resolved WL ambiguities are introduced to perform a narrow-lane (NL) ambiguity resolution on the basis of the ionosphere-free linear combination (L3). Taking the baselines HUBF (77.4 km) and WTHU (416.6 km) as examples, Fig. 4 shows the percentages of the resolved ambiguities with respect to observation weighting and baseline length.

FIGURE 4

From both graphs it can be seen that more WL ambiguities are resolved than NL ambiguities, which is attributed to the significantly larger WL wavelength of about 86 cm in comparison to the NL wavelength of about 11 cm (Dach et al., 2007, pp. 40, 41). For the short baseline HUBF, the WL ambiguity resolution is only insignificantly affected by the use of EXPZ, while it experiences an average improvement of nearly 10% for the long baseline WTHU. In terms of NL ambiguity resolution, the results are enhanced by up to about 10% for both baselines if the conventional COSZ model is replaced by the advanced EXPZ scheme. For the longer baseline WTHU, the percentages of the resolved ambiguities are smaller, and the benefits of applying EXPZ instead of COSZ are more obvious.

Considering all baselines analysed in this study, Table 3 presents the overall results of ambiguity resolution using different observation weighting schemes. Applying the COSZ and EXPZ models to the same data set, the number of total ambiguities (#AMB) can be slightly different (see HUBF and WTBF), which originates from the residual-based outlier detection and observation deletion (Dach et al., 2007, pp. 133, 145). In comparison to COSZ, the employment of EXPZ improves the average success rates of WL and NL ambiguity resolution by up to 9.4 and 7.9%, respectively. The corresponding

Table 3: Results of ambiguity resolution using different observation weighting models (#/%: number/percentage of resolved ambiguities).

Analysed baseline	**Length** [km]	**COSZ** [#/%]			**EXPZ** [#/%]			**Increase WL** [%]		**Increase NL** [%]	
		#AMB	WL	NL	#AMB	WL	NL	Mean	Max	Mean	Max
HUBF	77.4	**385**	380/98.7	337/87.5	**387**	382/98.7	360/93.0	0.0	1.9	5.5	9.0
ZIHU	106.9	373	354/94.9	329/88.2	373	365/97.9	345/92.5	3.0	4.9	4.3	8.2
ZIBF	174.1	309	285/92.2	262/84.8	309	295/95.5	272/88.0	3.3	5.6	3.2	7.6
WTBF	346.9	**381**	316/82.9	294/77.2	**383**	348/90.9	312/81.5	8.0	11.4	4.3	7.5
WTHU	416.6	469	375/80.0	341/72.7	469	415/88.5	378/80.6	8.5	**13.5**	**7.9**	9.3
ZIWT	475.9	382	301/78.8	286/74.9	382	337/88.2	303/79.3	**9.4**	12.3	4.4	**12.3**

maximum daily enhancements are 13.5 and 12.3%. In addition, as the baseline length increases, the performance of ambiguity resolution degrades, and the EXPZ model becomes more beneficial (see the grey-marked column of Table 3). An average improvement of 10% in ambiguity resolution was also achieved by means of the ESNR approach (Luo et al., 2008a,c; Luo, 2013, Chap. 6), verifying the sufficiency of the EXPZ method in characterising the empirical SNR-based weights (see Eq. (1) and Fig. 1).

4.2. Effects on troposphere parameter estimation

GPS signals are delayed while propagating through the Earth's troposphere. In the zenithal direction, the tropospheric delay amounts to about 2.3 m at sea level (Hofmann-Wellenhof et al., 2008, p. 135). Analysing GPS observations with the Bernese GPS Software 5.0, this delay term can be evaluated by estimating site-specific troposphere parameters (TRP; Dach et al., 2007, Chap. 11). The quality of the parameter estimates is affected by various factors, e.g., observation weighting (Luo et al., 2008b). The TRP estimates have a temporal resolution of 1 h (i.e., 24 parameters per day per station) and are obtained from network solutions by stacking the normal equations. Since data from elevations below 10° are included, horizontal tropospheric gradients are determined on a daily basis to account for the azimuthal asymmetry of the local troposphere at the observation site (Meindl et al., 2004; Dach et al., 2007, Sect. 11.4.3). For the IGS station WTZR, Fig. 5 shows the TRP estimates and the associated standard deviations (STD) from the daily and weekly network solutions using different weighting models.

FIGURE 5

Regarding the results of the daily network solutions (see Fig. 5a and b), the use of EXPZ instead of COSZ leads to considerable changes in the TRP estimates of up to 6 cm and a mean decrease in the corresponding STD (ΔSTD) of 1.7 mm (45%). The differences in TRP are mostly negative, which was also found in Jin and Park (2005). Considering the increased σ_0 from COSZ to EXPZ, the decreases in STD are caused by the larger observation weights, particularly at low elevation angles (see Fig. 2). Similar behaviour was observed in Luo et al. (2008b) when comparing the equal weight and COSZ models. The daily solutions exhibit jumps in both the TRP (e.g., days 302 and 307 in Fig. 5a) and the STD estimates (e.g., days 304 and 305 in Fig. 5b), which, however, disappear in the weekly solutions (see Fig. 5c and d). In this case, the application of EXPZ changes the TRP by as much as 4 cm and reduces the STD by 1.0 mm (40%) on average.

Table 4 presents the overall results of the TRP estimation using different observation weighting models. For both the daily and weekly solutions, cm-level root mean squares (RMS) of the differences between TRP(COSZ) and TRP(EXPZ) are obtained. Moreover, applying the EXPZ scheme, the TRP values of IGS sites WTZR and ZIMM are closer to the CODE products. Being superior to COSZ, the EXPZ model improves the TRP precision by up to 1.7 mm absolutely and 45% relatively, where the daily solutions experience stronger benefits. Similar magnitudes of enhancements, achieved by means of advanced stochastic models, were reported by Jin and Park (2005) and Jin et al. (2010). With the context of GPS meteorology, cm-level changes in TRP and mm-level improvements in STD are already significant (Bender et al., 2008; Fuhrmann et al., 2010, Sect. 8.3).

Table 4: Results of troposphere parameter estimation using different weighting models.

Station	**Height**	**Daily solution**		**Weekly solution**	
	[m]	RMS [cm]	ΔSTD [mm/%]	RMS [cm]	ΔSTD [mm/%]
HUEG	278.3	1.6	1.7/44	1.2	1.0/39
WTZR	666.0	1.6	**1.7/45**	1.4	1.0/39
BFO1	690.3	1.8	1.7/43	1.5	0.9/37
ZIMM	956.3	1.7	1.6/44	1.4	0.9/39

4.3. Effects on site coordinate determination

The effects of EXPZ on site coordinate (CRD) determination are assessed by examining the differences and increments of the coordinate estimates from daily network solutions. For the IGS sites WTZR and ZIMM, Fig. 6 illustrates the absolute differences between the coordinates from COSZ and EXPZ, as well as the height increments in a local topocentric system. As could be expected, Fig. 6a and b depict insignificant coordinate differences of less than 1 mm in the horizontal components northing (N) and easting (E), while considerably larger deviations of up to 8 mm are detected in the height (H) component (see WTZR). From both graphs it can be seen that more significant height differences are present on day 304, which can be explained by the fact that only about 2 hours of ZIMM data, i.e., from 00:00:00 to 01:56:30, were available on this particular day. Regarding the associated height increments shown in Fig. 6c and d, the use of EXPZ instead of COSZ improves the height repeatability, especially on day 304 (cf. Fig. 6a and b). For WTZR and ZIMM, the RMS values of the height increments are decreased by 1.4 and 2.3 mm, respectively, indicating a more reliable determination of the vertical component.

FIGURE 6

316 Table 5 presents the median and maximum absolute coordinate differences
317 caused by applying different observation weighting models. The median val-
318 ues are predominantly less than 1 mm in the horizontal components, but
319 can reach up to about 7 mm in the vertical component (see BFO1). The
320 maximum changes in the northing and easting coordinates amount to a few
321 mm, while a maximum height difference of 1.5 cm is detected on day 304 for
322 BFO1. This large deviation arises not only from the limited ZIMM data on
323 this particular day, but also from the interference of GPS signals due to the
324 heavy vegetation (Luo and Mayer, 2008).

325 To investigate the influence of EXPZ on coordinate repeatability, the
326 RMS values of the daily coordinate increments are presented in Table 6. Ex-
327 amining the magnitudes of the RMS first, the maximum is less than 2 mm for
328 the horizontal components and 5 mm for the vertical. The small RMS values
329 verify the high performance of the GPS data analysis using the Bernese GPS
330 Software 5.0 (see Table 2). Furthermore, the easting coordinates appear to
331 be more precise than the northing, which is due to the so-called "north hole".
332 Although the proposed EXPZ model degrades the horizontal coordinate re-
333 peatability by up to 0.6 mm, it improves the height precision by as much as
334 2.3 mm (50%).

335 Table 5: Median (Med) and maximum (Max) absolute topocentric coordinate differences in mm caused by applying the observation weighting models COSZ and EXPZ.

Station	**Height**	**Northing** $\lvert\Delta N\rvert$		**Easting** $\lvert\Delta E\rvert$		**Height** $\lvert\Delta H\rvert$	
	[m]	Med	Max	Med	Max	Med	Max
HUEG	278.3	0.4	0.8	0.2	0.6	2.0	4.4
WTZR	666.0	0.4	1.1	0.7	1.0	2.1	7.8
BFO1	690.3	0.5	1.3	2.0	3.4	**6.6**	**15.0**
ZIMM	956.3	0.3	0.9	0.5	1.0	1.8	5.9

Table 6: Root mean square (RMS) values of the daily coordinate increments in mm.

Station	**Height**	**COSZ**			**EXPZ**			**Decrease**		
	[m]	N	E	H	N	E	H	N	E	H
HUEG	278.3	0.6	0.4	1.4	0.8	0.6	2.0	−0.2	−0.2	−0.6
WTZR	666.0	0.5	0.4	3.9	1.1	0.9	2.5	**−0.6**	−0.5	1.4
BFO1	690.3	0.8	0.8	3.5	1.4	1.2	3.4	**−0.6**	−0.4	0.1
ZIMM	956.3	1.2	0.7	**4.5**	**1.6**	1.1	2.2	−0.4	−0.4	**2.3**

5. Conclusions and outlook

On the basis of the empirical SNR-based weighting model proposed by Luo et al. (2008a,c), this paper presented a realistic and easy-to-implement weighting scheme for GPS phase observations. It uses the exponential function provided by Euler and Goad (1991) and is denoted as EXPZ. The model parameters are derived in an ad-hoc manner by approximating the mean elevation-dependent characteristics of representative empirical SNR-based weights. Analysing GPS data from a regional network, the EXPZ scheme is compared with the COSZ model implemented by default in the scientific Bernese GPS Software 5.0 (Dach et al., 2007, p. 144). The main findings of this study are summarised as follows:

1. The EXPZ model sufficiently captures the elevation-dependent properties of the empirical SNR-based weights. Differing from COSZ, it produces larger weights for low- and medium-elevation observations, increasing their contributions to GPS parameter estimation.
2. Using EXPZ instead of COSZ to resolve double-difference ambiguities, an average improvement of 10% in wide-lane and narrow-lane ambiguity resolution can be achieved, particularly for long baselines of several hundred kilometres.

3. A switch from COSZ to EXPZ may lead to cm-level changes in the estimated site-specific troposphere parameters and mm-level (i.e., about 40%) decreases in the associated standard deviations.
4. Under weak multipath and calm atmospheric conditions, the use of EXPZ instead of COSZ results in coordinate changes of less than 5 mm. When analysing short-term and low-quality data, the EXPZ model may significantly improve coordinate estimates at the centimetre level.
5. Within the framework of the presented case study, using EXPZ to specify larger weights for low- and medium-elevation observations degrades the horizontal coordinate repeatability by as much as 0.6 mm, but enhances the height precision by up to 2.3 mm.

Future research work will focus on the verification and refinement of the EXPZ model. For example, apart from static relative positioning, precise point positioning and kinematic data processing can be performed. By applying EXPZ to GLONASS, Galileo, or BeiDou measurements, the model efficiency can be assessed in a more generic GNSS sense. Instead of an ad-hoc approach, a rigorous determination of the model parameters is recommended, which may be carried out considering the receiver and antenna types. Moreover, a comparison of the refined EXPZ model with other observation weighting schemes is also planned.

Acknowledgements

The research project has been funded by the German Research Foundation (DFG Project No. HE 1433/16-2). J. L. Awange appreciates the financial support from the Alexander von Humboldt Foundation (Ludwig Leichhardt's

Memorial Fellowship) and the Curtin Research Fellowship. He is grateful to his host Prof. B. Heck for the enjoyable working atmosphere at the Geodetic Institute, Karlsruhe Institute of Technology (KIT). Two anonymous reviewers are deeply acknowledged for their valuable comments.

References

Amiri-Simkooei, A. R., Teunissen, P. J. G., and Tiberius, C. C. J. M. (2009). Application of least-squares variance component estimation to GPS observables. *J. Surv. Eng.*, 135(4):149–160. doi:10.1061/(ASCE)0733-9453(2009)135:4(149).

Bender, M., Dick, G., Wickert, J., Schmidt, T., Song, S., Gendt, G., Ge, M., and Rothacher, M. (2008). Validation of GPS slant delays using water vapour radiometers and weather models. *Meteorol. Z.*, 17(6):807–812. doi:10.1127/0941-2948/2008/0341.

Bischoff, W., Heck, B., Howind, J., and Teusch, A. (2005). A procedure for testing the assumption of homoscedasticity in least squares residuals: A case study of GPS carrier-phase observations. *J. Geod.*, 78(7–8):397–404. doi:10.1007/s00190-004-0390-5.

Brunner, F. K., Hartinger, H., and Troyer, L. (1999). GPS signal diffraction modelling: The stochastic SIGMA-Δ model. *J. Geod.*, 73(5):259–267. doi:10.1007/s001900050242.

Butsch, F. (2002). A growing concern: Radiofrequency interference and GPS. *GPS World*, 13(10):40–50.

Butsch, F. and Kipka, A. (2004). Die Bedeutung des Signal- zu Rauschleistungsverhältnisses und verwandter Parameter für die Messgenauigkeit bei GPS. *Allgemeine Vermessungs-Nachrichten (AVN)*, 111(2):46–55.

Collins, J. P. and Langley, R. B. (1999). Possible weighting schemes for GPS carrier phase observations in the presence of multipath. Final contract report for the United States Army Corps of Engineers Topographic Engineering Center, No. DAAH04-96-C-0086/TCN 98151, Department of Geodesy and Geomatics Engineering, University of New Brunswick (UNB), New Brunswick, Canada.

Collins, J. P. and Stewart, P. (1999). GPS SNR observations. Internal memorandum, 21 July, Geodetic Research Laboratory, University of New Brunswick (UNB), Fredericton, Canada.

Dach, R., Hugentobler, U., Fridez, P., and Meindl, M. (2007). Bernese GPS Software Version 5.0. Astronomical Institute, University of Bern, Stämpfli Publications AG, Bern, Switzerland.

Euler, H.-J. and Goad, C. C. (1991). On optimal filtering of GPS dual frequency observations without using orbit information. *Bull. Geod.*, 65(2):130–143. doi:10.1007/BF00806368.

Fuhrmann, T., Knöpfler, A., Mayer, M., Luo, X., and Heck, B. (2010). Zur GNSS-basierten Bestimmung des atmosphärischen Wasserdampfgehalts mittels Precise Point Positioning. Schriftenreihe des Studiengangs Geodäsie und Geoinformatik, Band 2/2010, Karlsruhe Institute of Technology (KIT), KIT Scientific Publishing, Karlsruhe, Germany.

425 Han, S. (1997). Quality-control issues relating to instantaneous ambiguity
426 resolution for real-time GPS kinematic positioning. *J. Geod.*, 71(6):351–
427 361. doi:10.1007/s001900050103.

428 Hartinger, H. and Brunner, F. K. (1999). Variances of GPS
429 phase observations: The SIGMA-ϵ model. *GPS Solut.*, 2(4):35–43.
430 doi:10.1007/PL00012765.

431 Hofmann-Wellenhof, B., Lichtenegger, H., and Wasle, E. (2008). *GNSS-*
432 *Global Navigation Satellite Systems: GPS, GLONASS, Galileo & more.*
433 Springer-Verlag, Wien.

434 Howind, J. (2005). Analyse des stochastischen Modells von GPS-
435 Trägerphasenbeobachtungen. Deutsche Geodätische Kommission,
436 No. C584, Verlag der Bayerischen Akademie der Wissenschaften, Munich.

437 Jin, S. G., Luo, O., and Ren, C. (2010). Effects of physical correlations
438 on long-distance GPS positioning and zenith tropospheric delay estimates.
439 *Adv. Space Res.*, 46(2):190–195. doi:10.1016/j.asr.2010.01.017.

440 Jin, S. G. and Park, P. H. (2005). A new precision improvement in zenith
441 tropospheric delay estimation by GPS. *Curr. Sci.*, 89(6):997–1000.

442 Joseph, A. (2010). GNSS solutions: What is the difference between SNR and
443 C/N_0? *Inside GNSS*, 5(8):20–25.

444 Kim, D. and Langley, R. B. (2001). Quality control techniques and issues
445 in GPS applications: Stochastic modelling and reliability testing. In: Pro-
446 ceedings of the 8th GNSS Workshop – 2001 International Symposium on

GPS/GNSS, Jeju, Korea, November 7–9, 2001, Tutorial/Domestic Session, pp. 76–85.

King, R. W. and Bock, Y. (2002). Documentation for the GAMIT GPS Analysis Software, Release 10.0. Massachusetts Institute of Technology (MIT), Cambridge, MA, USA.

Langley, R. B. (1997). GPS receiver system noise. *GPS World*, 8(6):40–45.

Li, B., Shen, Y., and Xu, P. (2008). Assessment of stochastic models for GPS measurements with different types of receivers. *Chinese Sci. Bull.*, 53(20):3219–3225. doi:10.1007/s11434-008-0293-6.

Luo, X. (2013). *GPS Stochastic Modelling – Signal Quality Measures and ARMA Processes*. Springer Theses: Recognizing Outstanding Ph.D. Research. Springer-Verlag, Berlin Heidelberg (in production).

Luo, X. and Mayer, M. (2008). Automatisiertes GNSS-basiertes Bewegungsmonitoring am Black Forest Observatory (BFO) in Nahezu-Echtzeit. *Zeitschrift für Geodäsie, Geoinformation und Landmanagement (ZfV)*, 133(5):283–294.

Luo, X., Mayer, M., and Heck, B. (2007). Quantifizierung verschiedener Einflussfaktoren in GNSS-Residuen. *Zeitschrift für Geodäsie, Geoinformation und Landmanagement (ZfV)*, 132(2):97–107.

Luo, X., Mayer, M., and Heck, B. (2008a). Erweiterung des stochastischen Modells von GNSS-Beobachtungen unter Verwendung der Signalqualität. *Zeitschrift für Geodäsie, Geoinformation und Landmanagement (ZfV)*, 133(2):98–107.

Luo, X., Mayer, M., and Heck, B. (2008b). Impact of various factors on the quality of site-specific neutrospheric parameters within GNSS data processing: A case study. *Bol. Ciênc. Geod.*, 14(4):461–481.

Luo, X., Mayer, M., and Heck, B. (2008c). Improving the stochastic model of GNSS observations by means of SNR-based weighting. In: M. G. Sideris (ed.), *Observing our Changing Earth*, Proceedings of the 2007 IAG General Assembly, Perugia, Italy, July 2–13, IAG Symposia, Vol. 133, Springer-Verlag, Berlin Heidelberg, pp. 725–734. doi:10.1007/978-3-540-85426-5_83.

Mayer, M. (2006). Modellbildung für die Auswertung von GPS-Messungen im Bereich der Antarktischen Halbinsel. Deutsche Geodätische Kommission, No. C597, Verlag der Bayerischen Akademie der Wissenschaften, Munich.

Meindl, M., Schaer, S., Hugentobler, U., and Beutler, G. (2004). Tropospheric gradient estimation at CODE: Results from global solutions. *J. Meteorol. Soc. Jpn.*, 82(1B):331–338. doi:10.2151/jmsj.2004.331.

Niell, A. E. (1996). Global mapping functions for the atmosphere delay at radio wavelengths. *J. Geophys. Res.*, 101(B2):3227–3246. doi:10.1029/95JB03048.

Saastamoinen, J. (1973). Contribution to the theory of atmospheric refraction: Part II. Refraction corrections in satellite geodesy. *Bull. Geod.*, 107(1):13–34. doi:10.1007/BF02522083.

Satirapod, C. and Luansang, M. (2008). Comparing stochastic model used in GPS precise point positioning technique. *Surv. Rev.*, 40(308):188–194. doi:10.1179/003962608X290988.

493 Schmid, R., Steigenberger, P., Gendt, G., Ge, M., and Rothacher, M.
494 (2007). Generation of a consistent absolute phase-center correction
495 model for GPS receiver and satellite antennas. *J. Geod.*, 81(12):781–798.
496 doi:10.1007/s00190-007-0148-y.

497 Schön, S. and Brunner, F. K. (2008). A proposal for modelling physi-
498 cal correlations of GPS phase observations. *J. Geod.*, 82(10):601–612.
499 doi:10.1007/s00190-008-0211-3.

500 Teunissen, P. J. G., Jonkman, N. F., and Tiberius, C. C. J. M. (1998).
501 Weighting GPS dual frequency observations: Bearing the cross of cross-
502 correlation. *GPS Solut.*, 2(2):28–37. doi:10.1007/PL00000033.

503 Wieser, A. (2007). GNSS solutions: How important is GNSS observation
504 weighting? *Inside GNSS*, 2(1):26–28.

505 Wieser, A. and Brunner, F. K. (2000). An extended weight model for GPS
506 phase observations. *Earth Planets Space*, 52(10):777–782.

507 Wieser, A. and Brunner, F. K. (2002). Short static GPS sessions: Robust
508 estimation results. *GPS Solut.*, 5(3):70–79. doi:10.1007/PL00012901.

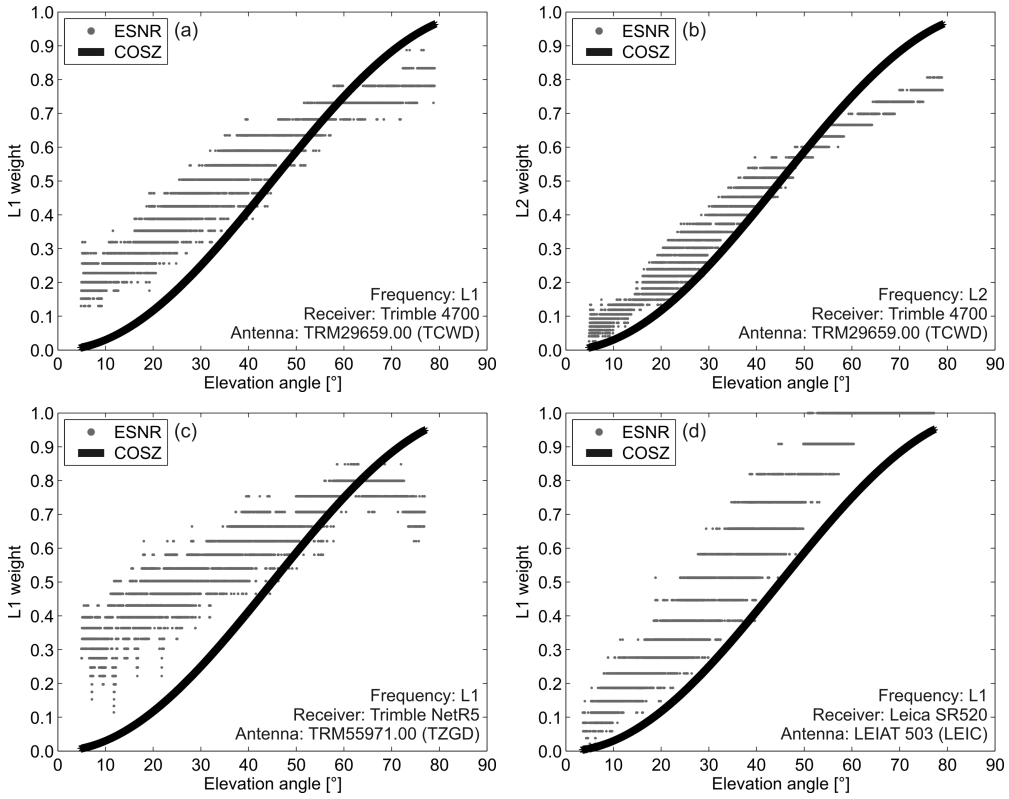

Figure 1: Comparison of the phase observation weights produced by different weighting schemes (ESNR: empirical SNR-based, $a = 0.1$, see Eq. (1); COSZ: elevation-dependent, see Eq. (2); TCWD, TZGD, LEIC: antenna radomes).

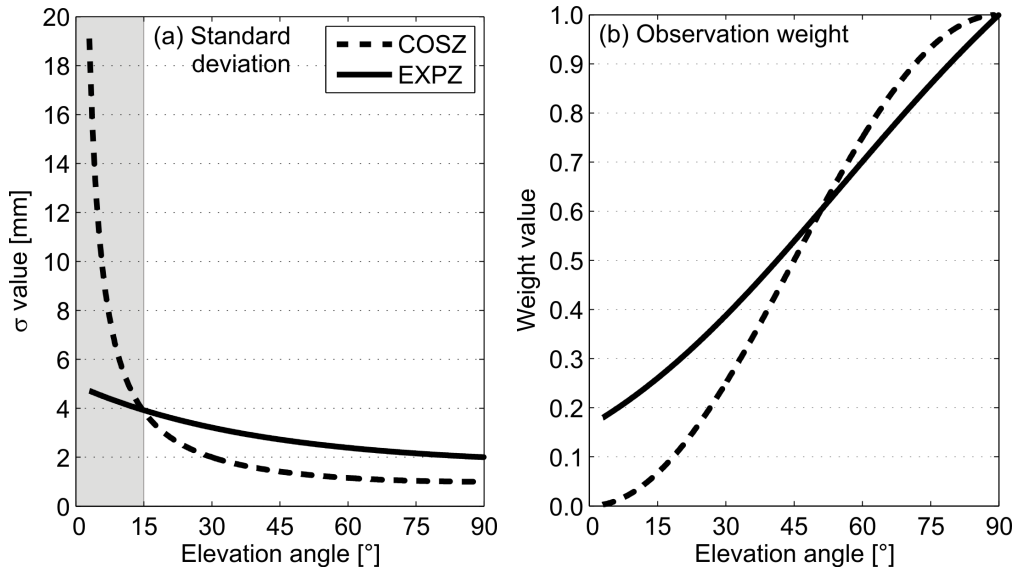

Figure 2: Comparison of the standard deviations (a) and observation weights (b) produced by the COSZ ($\sigma_0 = 1$ mm, see Eq. (2); Dach et al., 2007, p. 144) and EXPZ ($\sigma_0 = 2$ mm, see Eqs. (3)–(4); Hofmann-Wellenhof et al., 2008, p. 108) models.

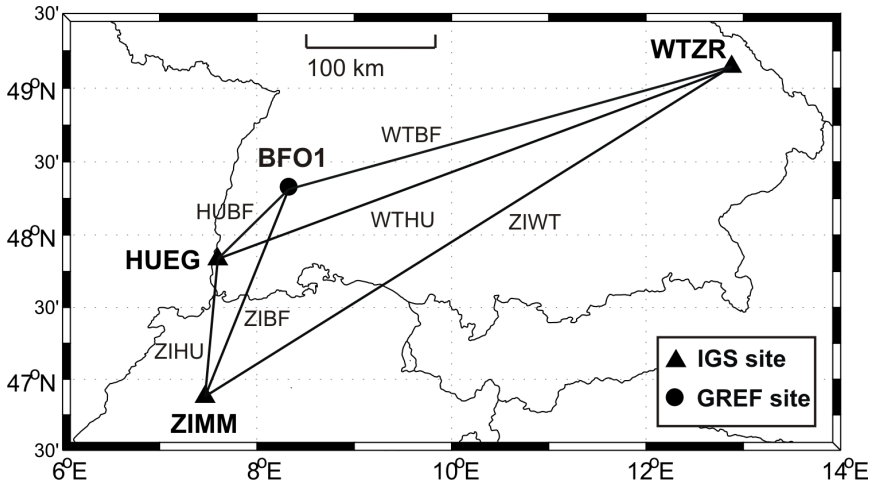

Figure 3: Regional network design and baseline creation (see Table 1).

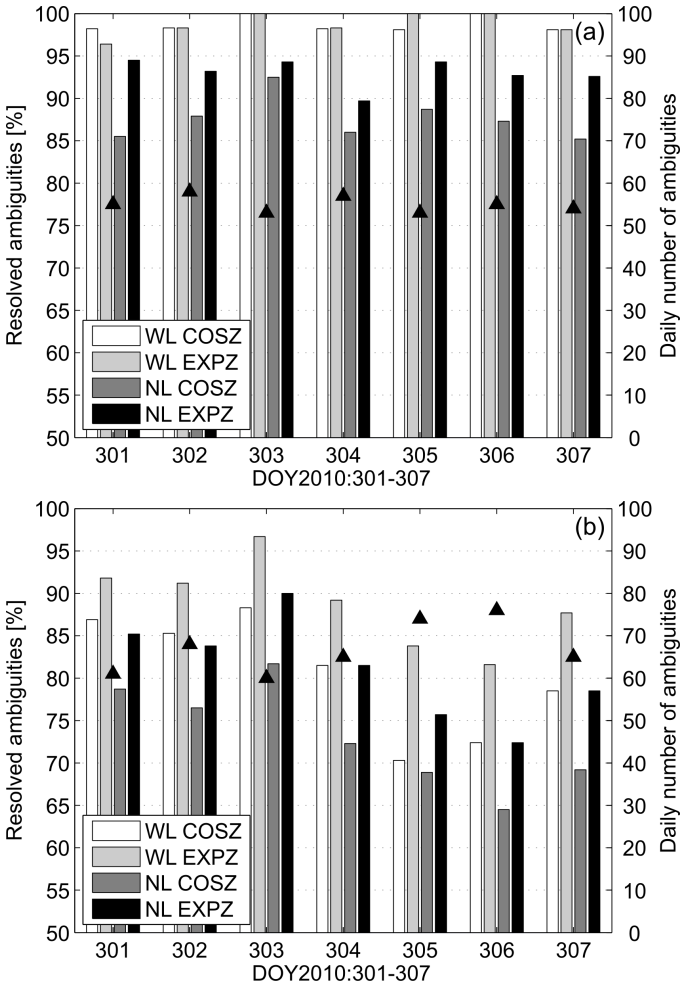

Figure 4: Examples of the results of phase ambiguity resolution with respect to observation weighting and baseline length (filled black triangle: daily number of ambiguities, see Table 1) (a) Short baseline HUBF: 77.4 km, (b) Long baseline WTHU: 416.6 km.

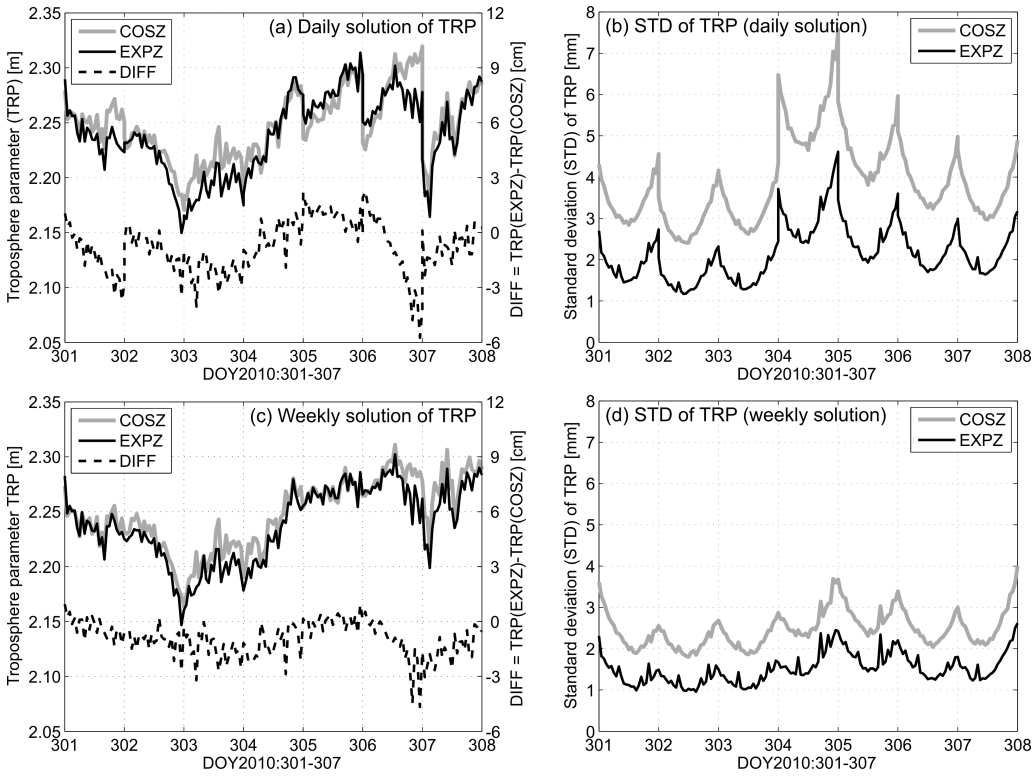

Figure 5: Examples of the results of troposphere parameter (TRP) estimation with respect to observation weighting (IGS site: WTZR, TRP time span: 1 h, STD: standard deviation).

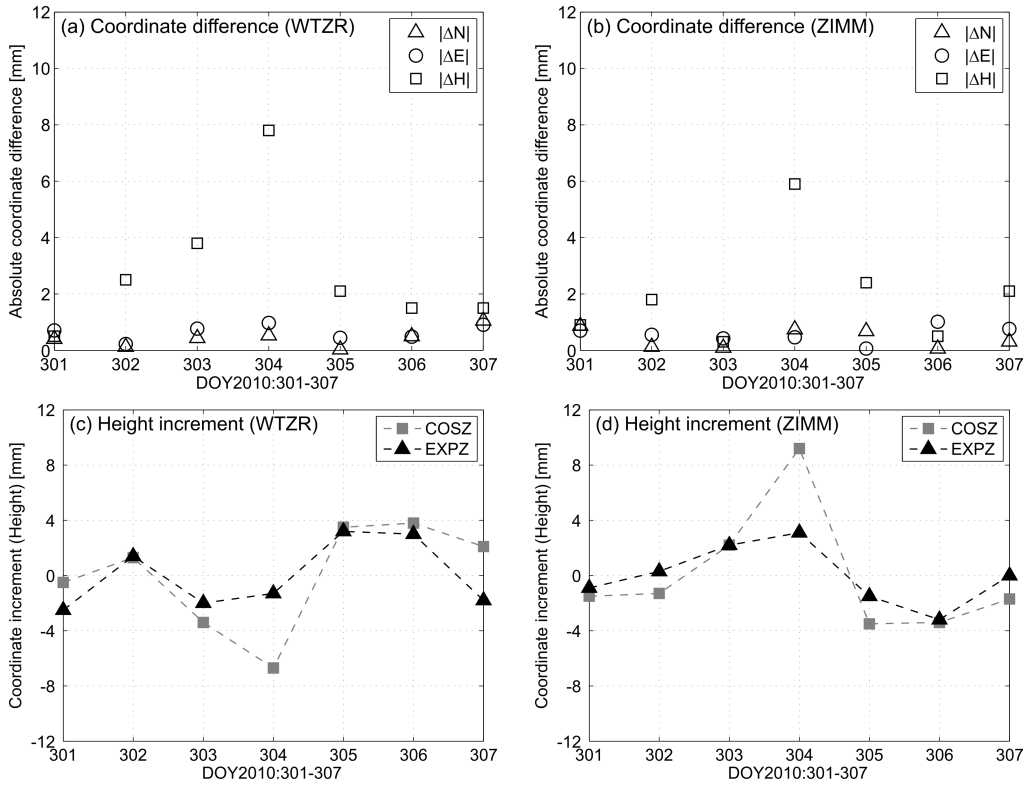

Figure 6: Examples of the results of site coordinate determination with respect to observation weighting (IGS sites: WTZR and ZIMM, daily network solutions).